Desalination and Water Treatment
www.deswater.com
doi: 10.1080/19443994.2015.1072060

57 (2016) 15026–15036
July

Taylor & Francis
Taylor & Francis Group

The potential application of tomato seeds as low-cost industrial waste in the adsorption of organic dye molecules from colored effluents

Hamed Najafi[a], Elmira Pajootan[b,*], Alireza Ebrahimi[b], Mokhtar Arami[b]

[a]*Department of Basic Science, Abhar Branch, Payam Nour University, Abhar, Iran, email: hamed.chem@gmail.com*
[b]*Textile Engineering Department, Amirkabir University of Technology, 424 Hafez Ave, Tehran 15875-4413, Iran, Tel. +98 2164542681; Fax: +98 2166400245; emails: pajootan@aut.ac.ir (E. Pajootan), reza.textile@aut.ac.ir (A. Ebrahimi), arami@aut.ac.ir (M. Arami)*

Received 14 February 2015; Accepted 2 July 2015

ABSTRACT

The objective of current study is to investigate the tomato seeds (TSs) as a low-cost industrial waste material to be employed in the adsorption of two acid dyes (C.I. Acid Red 14 (AR14) and C.I. Acid Blue 92 (AB92)). In this regard, field emission scanning electron microscope images, Fourier transform infrared analysis, and determination of isoelectric pH were used to characterize the surface morphology, functional groups, and surface charge of TS, respectively. Initial dye concentration, pH, and adsorbent dosage were studied as the key parameters that affect the adsorption performance. The isotherm, kinetic, and thermodynamic parameters of removal process were determined. It was found that the experimental data had followed the Langmuir isotherm model. The pseudo-second-order kinetic model described the rate of adsorption process properly. Temperature variation of adsorption process indicated that the removal of AR14 and AB92 by TS was an exothermic and spontaneous procedure. Finally, the cost analysis demonstrated that TS can be suggested as an effective and eco-friendly biosorbent for the removal of organic dyes from colored textile wastewaters.

Keywords: Tomato seed (TS); Low-cost adsorbent; Isotherm; Kinetic; Thermodynamic

1. Introduction

Textile is one of the most water contaminant industries due to its high water consumption. In recent years, it has become a remarkable subject for the researchers working on the environmental issues and wastewater treatment. Among the various processes in this industry, dyeing and finishing procedures are the main sources of wastewater production [1–3].

On the other hand, high toxicity, complex structures, synthetic nature, non-biodegradability, and the accumulation possibility of dye stuffs in the environment may cause serious health problems [4,5]. The extensive use of these hazardous compounds in many industries has focused the environmental concerns on the removal of dyes from effluents.

Various physical and chemical methods are available for the degradation or separation of contaminants from industrial wastewaters including coagulation and flocculation, ozonation, membrane filtration processes, ion exchange, chemical precipitation, etc.

*Corresponding author.

[3,6]. Adsorption is a preferable process to the other techniques due to its simple design, facile operation, and the ability to separate a wide range of compounds. Different types of materials with organic/mineral and natural/synthetic base are now being used as adsorbent in various studies [7,8]. Recently, many researches have been conducted to find available, effective, and low-cost materials like industrial and agricultural byproducts with the adsorption ability [2,3,9,10]. Various agricultural byproducts such as fern, rice husk, oak leaves [11], apple shell, orange peel, banana peel, millet waste [12], peach palm waste [13], coffee residues [14], and sugarcane bagasse [15] have been studied as adsorbent for the removal of different pollutants from wastewaters.

Tomato (*Lycopersicon esculentum* L) is grown throughout the world and it is used globally for human nutrition. Tomatoes are processed to produce ketchup, juices, paste, etc., which results in large amounts of tomato peel, pulp, fibrous matter, trimmings and seed as industrial wastes. These waste materials which contain 40% of the raw material are discharged into sewages and water streams [16–18].

In this study, the tomato seed (TS) as an agricultural low-cost byproduct is investigated for the removal of two acid dyes (C.I. Acid Red 14 and C.I. Acid Blue 92) from the colored wastewaters. The isoelectric pH (pH_{ZPC}, zero point charge) of TS was evaluated to determine the surface charge of the adsorbent. The functional groups and surface morphology of the adsorbent were studied by Fourier transform infrared (FTIR) spectra and field emission scanning electron microscope (FESEM) images, respectively. The effect of important parameters such as initial dye concentration, pH, adsorbent dosage, and temperature was investigated on the efficiency of the removal process. After the optimization of adsorption variables, isotherm, kinetic, and thermodynamic parameters were also studied to indicate the adsorption mechanism, rate constant, and spontaneous nature of the removal process. The desorption percentage of the dye-loaded adsorbent was also investigated. Moreover, the cost analysis of the adsorbent for the removal of dyes (1 g) from solution was carefully examined to evaluate the economic aspects of TS usage.

2. Materials and methods

2.1. Materials

TSs employed in this study were collected from the byproducts of a tomato paste factory in Iran. C.I. Acid Red 14 (AR14) and C.I. Acid Blue 92 (AB92) were supplied by Ciba Ltd (Table 1). Other chemicals were of analytical grade purchased from Merck.

2.2. Preparation of adsorbent

The TSs were separated from tomato waste and washed two times with distilled water and then dried in oven at 50˚C for 12 h. Then, the dried seeds were milled with a mortar and sieved to obtain the particle sizes lower than 250 μm.

2.3. Adsorption procedure

The dye solutions were prepared by dissolving a specific amount of dye in distilled water. H_2SO_4 (0.1 M) or NaOH (0.1 M) were used to adjust the pH of solutions.

The adsorption experiments (in batch mode) were performed on a magnetic stirrer at constant stirring rate of 200 rpm. The adsorption process was started by adding different dosages of TS (0.2–1.2 g/L) to 250-mL dye solution (50, 75, 100, 125, and 150 mg/L) at various pH values (3, 5, 7, 9, and 11) for 60 min at 30 ± 1˚C. Samples were taken from the solution at specified time intervals and centrifuged by Hettich EBA20 at 4,000 rpm for 10 min. The absorbance of solutions was measured using a vis spectrophotometer (Unico2100, China) at the maximum wavelength of each dye (515 and 572 nm for AR14 and AB92, respectively). The Dye removal efficiency was calculated using Eq. (1), in which A_0 and A refer to the absorbance at time = 0 and time = t, respectively [19]:

$$\text{Dye Removal Efficiency } (\%) = \left(\frac{A_0 - A}{A_0}\right) \times 100 \quad (1)$$

The adsorption capacity (q) which is defined as the amount of dye per unit mass of TS was calculated via Eq. (2):

$$q = \frac{(C_0 - C_e)V}{m} \quad (2)$$

where C_0 and C_e are the initial and equilibrium dye concentrations (mg/L) in bulk solution, m is the mass of adsorbent (g), and V is the volume of solution (L) [19].

2.4. Desorption studies

TS was collected and dried at room temperature after the adsorption of AR14 and AB92 (50 mg/L) for 60 min at pH 3. The dye-loaded adsorbent was added to 250-mL distilled water at pH values of 3, 5, 7, 9,

Table 1
Dyes' characteristics and structures

C.I. generic name	Molecular formula	Molecular weight (g/mol)
C.I. Acid Red 14 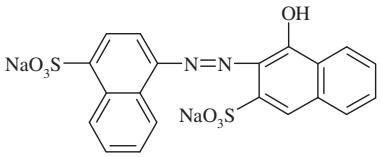	$C_{20}H_{12}N_2O_7S_2Na_2$	502.42
C.I. Acid Blue 92 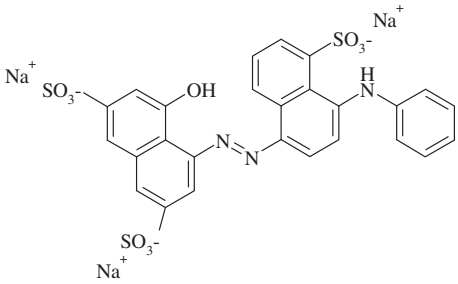	$C_{26}H_{16}N_3O_{10}S_3Na_3$	695.58

and 11. The fraction of dye molecules desorbed from TS was calculated using the Eq. (3) [20]:

$$\text{Desorption } (\%) = \left(\frac{\text{Amount released to solution } \left(\frac{\text{mg}}{\text{L}}\right)}{\text{Total adsorbed } \left(\frac{\text{mg}}{\text{L}}\right)}\right) \times 100 \quad (3)$$

2.5. Methods of characterization

The functional groups of TS were identified by FTIR spectroscopy. FTIR spectra were recorded with a Thermo Nicolet Avatar 360 FTIR Spectrometer within the range of 500–4000 cm^{-1}.

The surface morphology of TS was examined using a field emission scanning electron microscope ((FESEM) JSM-6700F, JEOL, Japan).

In order to determine the isoelectric pH (pH_{ZPC}) of the adsorbent, TS (1 g) was added to 50-mL KNO_3 solutions (0.01 M). The initial pH of solutions was adjusted from 2 to 11 using HNO_3 and NaOH. The solutions were stirred for 24 h and the final pH was recorded. The pH in which the value of ($pH_i - pH_f$) equals zero is known as pH_{ZPC} [1].

3. Results and discussion

3.1. Structural characterization of adsorbent

Electrostatic interactions between dye molecules and adsorbent initiate the adsorption process. In this regard, pH_{ZPC} of TS is determined and the results are shown in Fig. 1. It can be seen that pH_{ZPC} of TS is 4.5, indicating that the surface of the adsorbent is negatively charged at pH values above 4.5 and it is positively charged at pH < 4.5. Therefore, the attraction forces between the negative dye molecules and positive surface functional groups of the adsorbent can lead to the removal of AR14 and AB92 from the bulk solution.

FTIR spectra of TS, AR14 and TS after the adsorption of AR14 are given in Fig. 2. The FTIR spectra of TS after the adsorption of AR14 as the model dye was investigated to confirm that the adsorption process

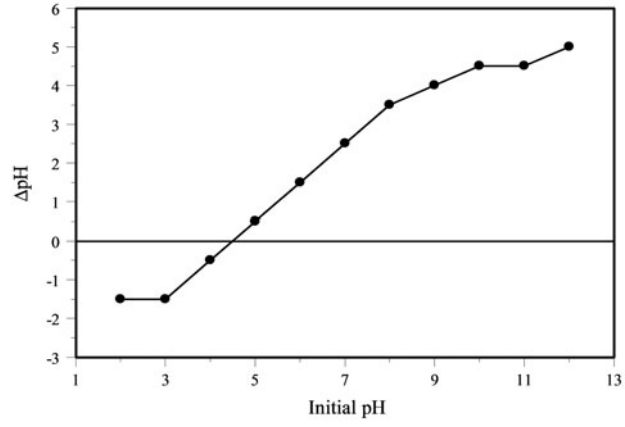

Fig. 1. pH_{ZPC} of TS.

has been performed successfully and there are evidences for bond formation between the adsorbent and dye molecules. The symmetric alkane C–H stretching bond is appeared at 2,925 and 2,850 cm^{-1}. The weak peak at 720 cm^{-1} can be assigned to the long chain bending bond in the structure of TS. The peaks appearing at 3,010, 1,460, and 650 cm^{-1} are corresponding to the alkene C–H stretching, bending, and out of plane (O O P) bending, respectively. The existence of secondary amide bond is confirmed by the appearance of peaks at 3,300, 1,659, 1,546, and 1,057 cm^{-1}, which can be attributed to the N–H stretching bond, C=O bond, N–H bending bond, and C–N bond, respectively. The O–H, C=O, and C–O bonds of carboxylic acid exhibited three peaks at 3,400, 1,711, and 1,247 cm^{-1}, respectively.

FTIR spectra of AR14 showed peaks at 3,438 cm^{-1} (O–H), 1,604 and 1,495 cm^{-1} (C=C), 1,189 cm^{-1} (C–N), 760 and 624 cm^{-1} (aromatic rings C–H groups). The decrease in the intensity of some peaks at 3,400, 3,300, 1,659, 1,546, 1,460, 1,247, and 1,057 cm^{-1} can be due to the involvement and interference of their corresponding functional groups in the adsorption of AR14 from aqueous solution.

The surface morphology of TS was studied by FESEM images (Fig. 3). According to this figure, two different structures (Fig. 3(a) and (b)): net-like and Fig. 3(c) and (d): rough and uneven) are observed for TS. Both of these structures have a porous surface with large surface area, which is one of the main characteristics of TS as an adsorbent for the removal of dye contaminants.

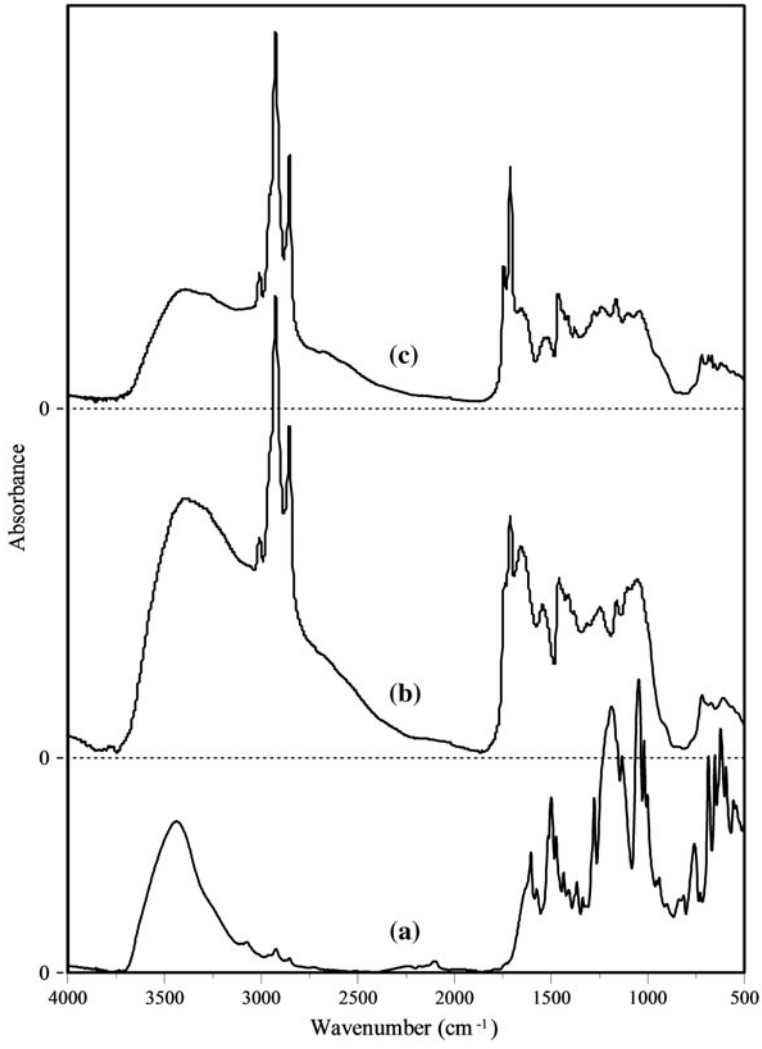

Fig. 2. FTIR spectra of (a) TS, (b) AR14, and (c) TS after the adsorption of AR14.

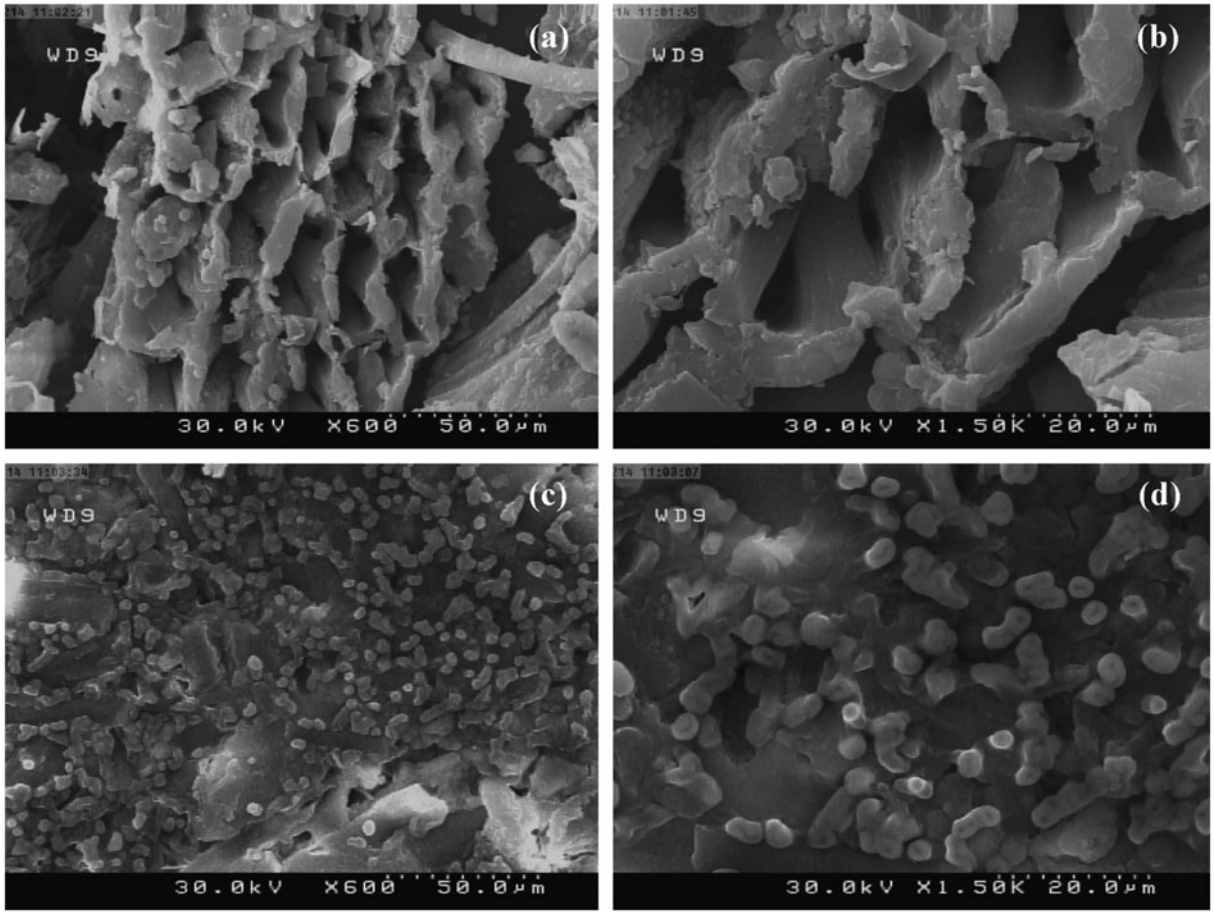

Fig. 3. FESEM images of the surface of TS at different magnifications.

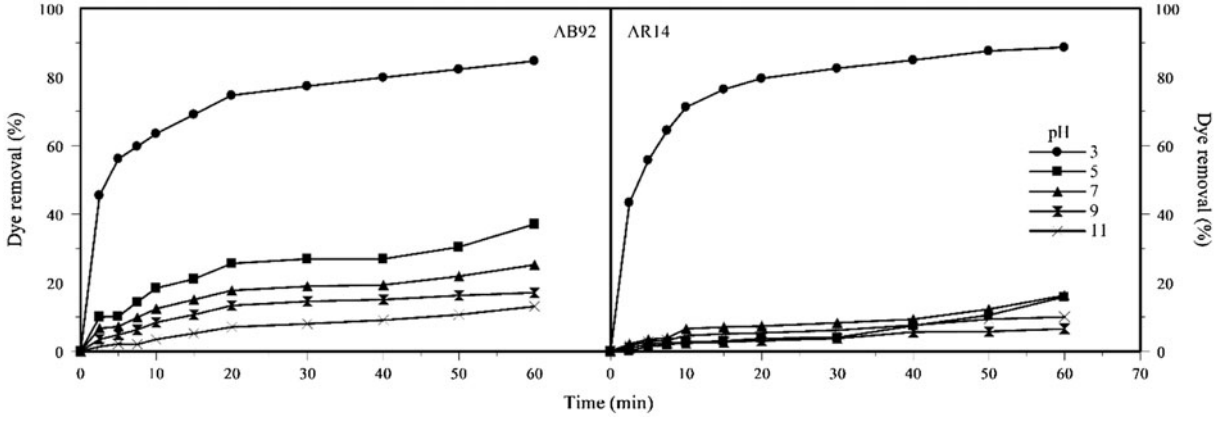

Fig. 4. Effect of pH on dye removal (%) ([C_0]: 50 mg/L, [TS]: 0.6 and 1.0 g/L for AR14 and AB92, *T*: 30˚C).

3.2. Effect of pH

Fig. 4 illustrates the effect of pH variation from 3 to 11 on the removal efficiency of AR14 and AB92 by TS. According to the results from pH_{ZPC} determination, the positively charged groups on the surface of TS are the dominant functional groups at low pH values and there is a strong electrostatic interaction between dye molecules and adsorbent, thus high values of removal (%) are achieved. But, in solutions at higher pH values, the number of negatively charged groups will increase and consequently, the repulsion forces between adsorbent and adsorbate will decrease the dye removal efficiency [1,21].

3.3. Effect of TS dosage

The effect of TS dosage on removal efficiency was investigated in the range of 0.2–0.8 g/L for AR14 and 0.6–1.2 g/L for AB92. According to the results in Fig. 5, by increasing the adsorbent dosage up to 0.6 and 1.0 g/L, the removal efficiency increases from 48 and 56% to 89 and 85% for AR14 and AB92, respectively. This can be attributed to the availability of more functional groups on the surface of TS, which results in the higher removal percentages of adsorption process. Further increasing of adsorbent dosage did not have a significant influence on the removal efficiency, so 0.6 and 1.0 g/L were chosen as the optimum values of TS dosage for the removal of AR14 and AB92, respectively. The trends of diagrams in Fig. 5 show that the adsorption process is fast at initial stage, but then it becomes slow due to the development of repulsion forces between the adsorbed dye molecules on the surface of TS and the remaining dyes in bulk solution [1].

3.4. Effect of initial dye concentration

Changes in initial dye concentration affect the efficiency of the removal process. So, the initial concentrations of AR14 and AB92 are varied from 50 to 150 mg/L at pH 3 and the results are exhibited in Fig. 6. Increase in the initial dye concentration results in the lower efficiencies of dye removal. When the concentration increases from 50 to 150 mg/L, the dye removal (%) decreases from 89 and 85% to 47 and 24% for AR14 and AB92, respectively. This can be attributed to the lower surface area of adsorbent in the presence of the constant amount of adsorbent [22,23].

3.5. Desorption studies

In order to study the regeneration possibility of TS to be used in more cycles of adsorption procedures and to keep the process cost down, 0.8 g/L of the previously dye-loaded adsorbent (at pH 3, TS dosages of 0.6 and 1.0 g/L for AR14 and AB92 and initial dye concentration of 50 mg/L) was added to 250-mL distilled water at various pH values (3–11). Desorption percentages are illustrated in Fig. 7. It can be seen that the dye-loaded adsorbent shows the highest desorption (%) of 57 and 63% for AR14 and AB92 at pH 11 due to the increasing of the negatively charged groups on the surface of TS, which facilitate the desorption of dye molecules by repulsion forces [1,24].

3.6. Equilibrium studies

3.6.1. Isotherm models

In this study, the Langmuir, Freundlich, and Temkin models were employed to analyze the

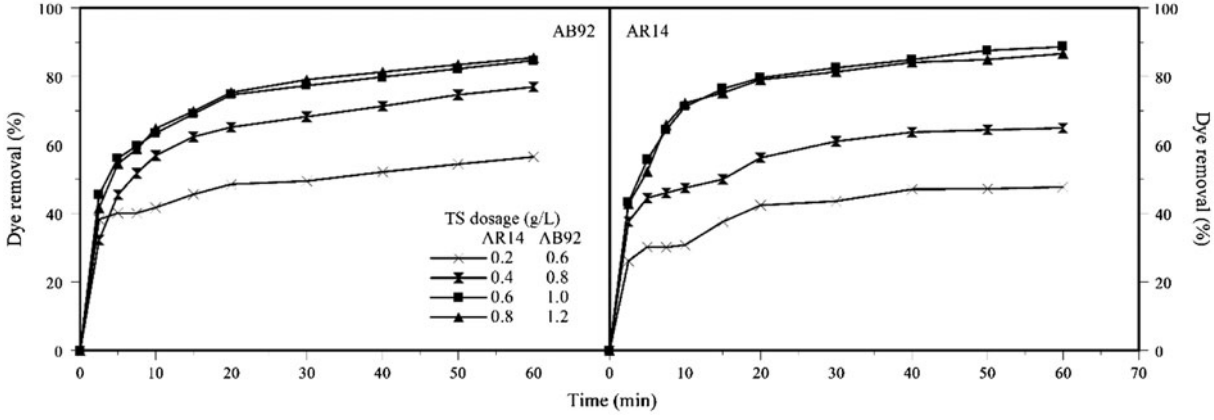

Fig. 5. Effect of adsorbent dosage on dye removal (%) ([C_0]: 50 mg/L, pH 3 and T: 30˚C).

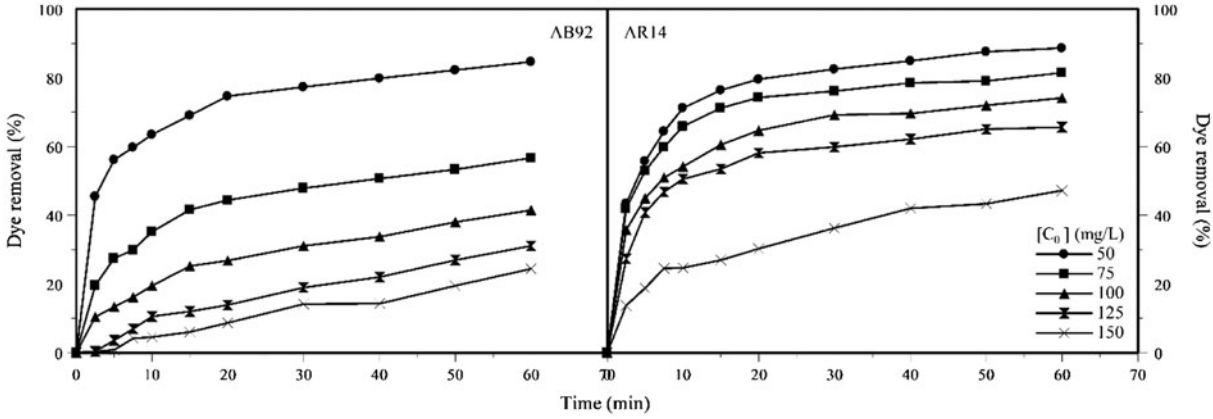

Fig. 6. Effect of initial dye concentration on dye removal (%) ([TS]: 0.6 and 1.0 g/L for AR14 and AB92, pH 3 and T: 30°C).

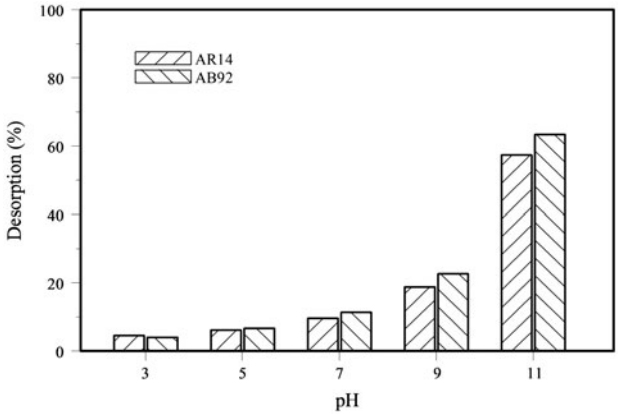

Fig. 7. Desorption (%) of AR14 and AB92 at various pH values ([TS]: 0.8 g/L and T: 30°C).

equilibrium data for designing a high-performance system. The monolayer coverage of the homogeneous surface of an adsorbent is the basic assumption of the Langmuir model. In this model, no interaction exists between the adsorbent available sites [25]. The linear Langmuir equation is given as Eq. (4):

$$C_e/q_e = (1/K_L q_m) + (C_e/q_m) \quad (4)$$

where q_e is AR14 or AB92 concentration on TS at equilibrium (mg/g), C_e is the equilibrium concentration of AR14 or AB92 in solution (mg/L), q_m is the maximum adsorption capacity of TS (mg/g), and K_L is the Langmuir constant (L/mg). Furthermore, the favorability of the adsorption process can be evaluated by the dimensionless separation factor (R_L) which is written as Eq. (5) [25,26]:

$$R_L = 1/(1 + K_L C_0) \quad (5)$$

where C_0 is the initial dye (AR14 or AB92) concentration (mg/L). The R_L values illustrate the type of isotherm to be unfavorable ($R_L > 1$), linear ($R_L = 1$), favorable ($0 < R_L < 1$), or irreversible ($R_L = 0$) [25,27].

Eq. (6) represents the linear form of the Freundlich isotherm with the homogeneous adsorbent surface along with the nonuniform distribution of the heat of adsorption over the surface. In this equation, K_F refers to the Freundlich constant ((mg/g) (L/mg)$^{1/n}$).

$$\log q_e = \log K_F + (1/n) \log C_e \quad (6)$$

Temkin isotherm expressed by Eq. (7) assumes that the reduction of heat of adsorption with the coverage is linear due to the interactions between the adsorbent and adsorbate.

$$q_e = B_T \ln K_T + B_T \ln C_e \quad (7)$$

$$B_T = RT/b \quad (8)$$

where B_T (mg/g) and K_T (L/mg) are the Temkin constants, T and R are the absolute temperature (K) and the universal gas constant (8.314 J/(mol K)), and b refers to the heat of adsorption. Table 2 contains the calculated parameters of the mentioned isotherm models with their correlation coefficients (R^2). High R^2 values confirm that the adsorption process using TS follows the Langmuir model and the surface of the adsorbent is covered with a monolayer of dye molecules. Also, the R_L values calculated by Eq. (5)

Table 2
Isotherm constants for the adsorption of AR14 and AB92 onto TS

	Langmuir			Freundlich			Temkin			
	q_m	K_L	R^2	log K_F	$1/n$	R^2	K_T	B_T	b	R^2
AR14	125.00	0.63	0.986	1.76	0.20	0.728	10.96	19.95	126.27	0.706
AB92	36.23	0.25	0.995	1.68	0.05	0.585	2.09	7.98	310.43	0.976

($0.01 < R_L < 0.08$) indicated the favorability of adsorption process.

3.6.2. Kinetic constants

Three kinetic equations including pseudo-first-order, pseudo-second-order, and intraparticle diffusion models were investigated to simulate the experimental data. Adsorption mechanism and its rate constant can be demonstrated by the process kinetics [28]. The pseudo-first and pseudo-second-order linear rate equations are written as follow:

$$\log (q_e - q_t) = \log (q_e) - (k_1/2.303)t \quad (9)$$

$$t/q_t = 1/k_2 q_e^2 + (1/q_e)t \quad (10)$$

where q_e and q_t are the amount of adsorbed dye at equilibrium and any time (mg/g), k_1 is the pseudo-first-order rate constant (1/min) and k_2 is the pseudo-second-order equilibrium rate constant (g/(mg min)) [29,30].

The obtained equilibrium data at various initial dye concentrations were also fitted to intraparticle diffusion rate model to survey the multilinearity of the adsorption process and to investigate the diffusion mechanism. Eq. (11) express the intraparticle diffusion model [8]:

$$q_t = k_p t^{0.5} + C \quad (11)$$

where k_p (mmol/(g s)) is the intraparticle diffusion rate constant and C is a constant dependent on the thickness of the boundary layer. The plots of log ($q_e - q_t$) vs. t, t/q_t vs. t and q_t vs. $t^{0.5}$at different dye concentrations were drawn and their slopes and intercepts were used to calculate the rate constants. These results and the experimental q_e values, coefficients of determination (R^2) and calculated q_e values are given in Table 3.

The results explore that the removal of AR14 and AB92 from colored solutions follows the pseudo-second-order kinetic model due to the highest correlation of coefficient (R^2) and close agreement between the experimental and calculated q_e values reported in Table 3.

The plots of q_t against $t^{0.5}$ were drawn and they were not linear, which indicated that the intraparticle diffusion was not involved in the adsorption process; and since the lines do not pass through the origin, this mechanism is not the rate-controlling step. This means that some level of boundary layer is involved in the adsorption, but the intraparticle diffusion is not the only rate-limiting step and other kinetic models control the adsorption process [31,32].

3.6.3. Thermodynamic parameters

Thermodynamic parameters of the adsorption process using TS including Gibbs free energy (ΔG), enthalpy (ΔH), and entropy (ΔS) were demonstrated by conducting the experiments at 30, 40, 50, and 60°C. The thermodynamic parameters were calculated by employing the Eqs. (12–14).

$$\Delta G = -RT \ln (q_e/C_e) \quad (12)$$

$$\ln (q_e/C_e) = (\Delta S/R) - (\Delta H/RT) \quad (13)$$

$$\Delta G = \Delta H - T\Delta S \quad (14)$$

where q_e is the concentration of adsorbed dye on TS at equilibrium (mg/g), C_e is the dye concentration in the solution (mg/L), R is the universal gas constant (8.314 J/(mol K)), and T is the absolute temperature (K). The slope and intercept of the plots of ln (q_e/C_e) vs. $1/T$ were used to determine ΔH and ΔS parameters. ΔG can also be calculated from Eq. (14) [33].

The resulted data from the effect of temperature on adsorption procedure are presented in Table 4. Negative values of ΔG are indicative of a spontaneous adsorption process. Moreover, negative values of ΔH and positive ΔS values show that the removal of AR14 and AB92 by TS is an exothermic reaction with

Table 3
Kinetic constants for the adsorption of AR14 and AB92 by TS

		Dye concentration (mg/L)									
		50		75		100		125		150	
		AR14	AB92	AR14	AB92	AR14	AB92	AR14	AB92	AR14	AB92
	$(q_e)_{exp}$ (mg/g)	73.822	42.327	101.696	42.476	123.541	41.405	136.568	38.830	117.716	36.495
Pseudo-first-order	$(q_e)_{cal}$ (mg/g)	42.024	22.646	49.238	30.095	70.990	35.793	88.982	41.210	99.687	39.875
	K_1 (1/min)	0.075	0.061	0.065	0.051	0.063	0.044	0.077	0.037	0.047	0.030
	R^2	0.950	0.939	0.904	0.966	0.943	0.977	0.937	0.965	0.976	0.950
Pseudo-second-order	$(q_e)_{cal}$ (mg/g)	76.336	43.29	104.167	44.444	126.582	45.045	140.845	50	125.000	57.143
	K_2 (g/mg min)	0.005	0.009	0.004	0.004	0.003	0.002	0.002	0.0007	0.001	0.0003
	R^2	0.998	0.997	0.998	0.988	0.997	0.956	0.997	0.775	0.965	0.456
Intraparticle diffusion	K_p (mg/g $s^{1/2}$)	7.958	4.409	10.697	5.025	13.489	5.201	15.195	5.328	14.296	4.904
	C	23.259	13.557	33.911	7.277	35.387	2.034	38.469	5.105	11.700	6.795
	R^2	0.774	0.78	0.750	0.922	0.816	0.988	0.806	0.968	0.974	0.925

Table 4
Thermodynamic parameters of the adsorption of AR14 and AB92 onto TS

	ΔG (kJ/mol)		ΔH (kJ/mol)		ΔS (kJ/mol K)	
T (K)	AR14	AB92	AR14	AB92	AR14	AB92
303	−6.45	−4.30	−7.23	−3.135	0.004	0.024
313	−5.09	−4.28				
323	−5.71	−4.85				
333	−6.18	−4.93				

increasing randomness at the interface of solid/liquid. Also, the obtained ΔG values are within the ranges of physisorption mechanisms ($-20 < \Delta G < 0$ kJ/mol) [34].

3.7. Cost analysis of TS

The cost analysis for TS is carried out to study its economic feasibility to employ for the removal of dye molecules from solutions. For this purpose, the cost associated to the preparation steps of adsorbent was carefully analyzed and reported in Table 5. It should be explained that 1 kg of dried TSs is approximately extracted from 83.3-kg tomato waste that includes water, peel, leaf, and seed. Then, the cost of adsorbent for the removal of 1 g of dye (AR14 and AB92) considering its adsorbent capacity was calculated and also presented in Table 5. The resulted data indicate that the utilized adsorbent is economically feasible (<0.12$ for the removal of 1 g dye molecule) and it can be classified as a low-cost adsorbent for the treatment

Table 5
Cost analysis of TS for the adsorption of AR14 and AB92

Cost of preparation of adsorbent ($/kg)		Total cost of adsorbent ($/kg)	Adsorbent capacity (mg/g)		Cost of adsorbent for removal of 1 g AR14 ($)	Cost of adsorbent for removal of 1 g AB92 ($)
			AR14	AB92		
Wet tomato waste (83.3 kg)	3.82	4.2845	125.00	36.23	0.034	0.118
Drying 1.99 kWh (50℃ for 12 h)	0.025					
Milling and sieving	0.05					
Net Cost ($)	3.895					
Other overhead costs (10% of net cost)	0.3895					

process of a colored effluent. This result may be owing to the fact that TS is a biodegradable waste byproduct from industrial activities and there is no chemical activation involved in the preparation of TS [35].

4. Conclusion

In this study, the effective removal of two acid dyes (C.I. Acid Red 14-AR14 and C.I. Acid Blue 92-AB92) was investigated using TS as a new natural and cost-effective biosorbent. The characterization of this adsorbent was analyzed by FTIR spectra, FESEM images, and pH_{ZPC} determination. The results indicated that TS with relatively porous surface area can be applicable for the removal of anionic dye molecules from the acidic media. In this regard, the effect of key factors such as adsorbent dosage, initial dye concentration, and pH was studied on the performance of TS for the removal of AR14 and AB92. The equilibrium data were analyzed by fitting them to various isotherm and kinetic models. The results showed that the Langmuir isotherm and pseudo-second-order kinetic models with highest R^2 values were best fitted to experimental data at various initial dye concentrations. According to thermodynamic investigation, the adsorption process was exothermic and spontaneous. The maximum dye removal of 89 and 85%, and maximum adsorption capacity of 125 and 36.23 (mg/g) were achieved for AR14 and AB92, respectively. The analysis of TS cost revealed that TS is economically feasible by showing the maximum cost of 0.118$ for the removal of 1-g dye investigated in this study. Therefore, TS can be successfully utilized as a low-cost, eco-friendly, and industrial waste material for the removal of organic dye molecules from effluents.

References

[1] L. Eskandarian, E. Pajootan, M. Arami, Novel super adsorbent molecules, carbon nanotubes modified by dendrimer miniature structure, for the removal of trace organic dyes, Ind. Eng. Chem. Res. 53(38) (2014) 14841–14853.

[2] A. Ebrahimi, M. Arami, H. Bahrami, E. Pajootan, Fish bone as a low-cost adsorbent for dye removal from wastewater: Response surface methodology and classical method, Environ. Model. Assess. 18 (2013) 1–10.

[3] A. Ebrahimi, E. Pajootan, M. Arami, H. Bahrami, Optimization, kinetics, equilibrium, and thermodynamic investigation of cationic dye adsorption on the fish bone, Desalin. Water Treat. 53 (2013) 1–11.

[4] E. Pajootan, M. Arami, N.M. Mahmoodi, Binary system dye removal by electrocoagulation from synthetic and real colored wastewaters, J. Taiwan Inst. Chem. Eng. 43(2) (2012) 282–290.

[5] E. Pajootan, M. Arami, M. Rahimdokht, Application of carbon nanotubes coated electrodes and immobilized TiO 2 for dye degradation in a continuous photocatalytic-electro-Fenton process, Ind. Eng. Chem. Res. 53 (42) (2014) 16261–16269.

[6] A.K. Mishra, T. Arockiadoss, S. Ramaprabhu, Study of removal of azo dye by functionalized multi walled carbon nanotubes, Chem. Eng. J. 162(3) (2010) 1026–1034.

[7] H. El Boujaady, M. Mourabet, M. Bennani-Ziatni, A. Taitai, Adsorption/desorption of Direct Yellow 28 on apatitic phosphate: Mechanism, kinetic and thermodynamic studies, J. Assoc. Arab Univ. Basic Appl. Sci. 16 (2014) 64–73.

[8] A. Roy, S. Chakraborty, S.P. Kundu, B. Adhikari, S.B. Majumder, Adsorption of anionic-azo dye from aqueous solution by lignocellulose-biomass jute fiber: Equilibrium, kinetics, and thermodynamics study, Ind. Eng. Chem. Res. 51(37) (2012) 12095–12106.

[9] A. Bousher, X. Shen, R.G.J. Edyvean, Removal of coloured organic matter by adsorption onto low-cost waste materials, Water Res. 31(8) (1997) 2084–2092.

[10] S. Chatterjee, A. Kumar, S. Basu, S. Dutta, Application of response surface methodology for Methylene Blue dye removal from aqueous solution using low cost adsorbent, Chem. Eng. J. 181–182 (2012) 289–299.

[11] E. Rosales, L. Ferreira, M.Á. Sanromán, T. Tavares, M. Pazos, Enhanced selective metal adsorption on optimised agroforestry waste mixtures, Bioresour. Technol. 182 (2015) 41–49.

[12] V. Okumuş, K.S. Çelik, S. Özdemir, A. Dündar, E. Kılınç, Biosorption of chlorophenoxy acid herbicides from aqueous solution by using low-cost agricultural wastes, Desalin. Water Treat. (2014) 1–10.

[13] A.P.A. Salvado, L.B. Campanholi, J.M. Fonseca, C.R.T. Tarley, J. Caetano, D.C. Dragunski, Lead(II) adsorption by peach palm waste, Desalin. Water Treat. 48(1–3) (2012) 335–343.

[14] C.-H. Wu, C.-Y. Kuo, S.-S. Guan, Adsorption of heavy metals from aqueous solutions by waste coffee residues: Kinetics, equilibrium, and thermodynamics, Desalin. Water Treat. (2015) 1–9.

[15] U.K. Garg, M.P. Kaur, V.K. Garg, D. Sud, Removal of Nickel(II) from aqueous solution by adsorption on agricultural waste biomass using a response surface methodological approach, Bioresour. Technol. 99(5) (2008) 1325–1331.

[16] D.S. Sogi, R. Bhatia, S.K. Garg, A.S. Bawa, Biological evaluation of tomato waste seed meals and protein concentrate, Food Chem. 89(1) (2005) 53–56.

[17] S. Machmudah, Zakaria, S. Winardi, M. Sasaki, M. Goto, N. Kusumoto, K. Hayakawa, Lycopene extraction from tomato peel by-product containing tomato seed using supercritical carbon dioxide, J. Food Eng. 108(2) (2012) 290–296.

[18] Y. Shi, Y. Zhang, H. Yao, J. Wu, H. Sun, H. Gong, Silicon improves seed germination and alleviates oxidative stress of bud seedlings in tomato under water deficit stress, Plant Physiol. Biochem. 78 (2014) 27–36.

[19] C. Kannan, K. Muthuraja, M.R. Devi, Hazardous dyes removal from aqueous solution over mesoporous aluminophosphate with textural porosity by adsorption, J. Hazard. Mater. 244–245 (2013) 10–20.

[20] S.A. Kosa, G. Al-Zhrani, M. Abdel Salam, Removal of heavy metals from aqueous solutions by multi-walled carbon nanotubes modified with 8-hydroxyquinoline, Chem. Eng. J. 181–182 (2012) 159–168.
[21] S. Li, Y. Gong, Y. Yang, C. He, L. Hu, L. Zhu, L. Sun, D. Shu, Recyclable CNTs/Fe_3O_4 magnetic nanocomposites as adsorbents to remove bisphenol A from water and their regeneration, Chem. Eng. J. 260 (2015) 231–239.
[22] Z. Chen, J. Zhang, J. Fu, M. Wang, X. Wang, R. Han, Q. Xu, Adsorption of methylene blue onto poly(cyclotriphosphazene-co-4,4´-sulfonyldiphenol) nanotubes: Kinetics, isotherm and thermodynamics analysis, J. Hazard. Mater. 273 (2014) 263–271.
[23] H. Yaacoubi, O. Zidani, M. Mouflih, M. Gourai, S. Sebti, Removal of cadmium from water using natural phosphate as adsorbent, Procedia Eng. 83 (2014) 386–393.
[24] S. Moharami, M. Jalali, Removal of phosphorus from aqueous solution by Iranian natural adsorbents, Chem. Eng. J. 223 (2013) 328–339.
[25] L. Eskandarian, M. Arami, E. Pajootan, Evaluation of adsorption characteristics of multiwalled carbon nanotubes modified by a poly(propylene imine) dendrimer in single and multiple dye solutions: isotherms, kinetics, and thermodynamics, J. Chem. Eng. Data 59(2) (2014) 444–454.
[26] C. Namasivayam, D. Kavitha, Removal of Congo Red from water by adsorption onto activated carbon prepared from coir pith, an agricultural solid waste, Dyes Pigm. 54(1) (2002) 47–58.
[27] M. Kumar, R. Tamilarasan, Kinetics and equilibrium studies on the removal of Victoria Blue using prosopis juliflora-modified carbon/Zn/alginate polymer composite beads, J. Chem. Eng. Data 58(3) (2013) 517–527.
[28] J.-Y. Tseng, C.-Y. Chang, C.-F. Chang, Y.-H. Chen, C.-C. Chang, D.-R. Ji, C.-Y. Chiu, P.-C. Chiang, Kinetics and equilibrium of desorption removal of copper from magnetic polymer adsorbent, J. Hazard. Mater. 171(1–3) (2009) 370–377.
[29] J.-G. Yu, X.-H. Zhao, H. Yang, X.-H. Chen, Q. Yang, L.-Y. Yu, J.-H. Jiang, X.-Q. Chen, Aqueous adsorption and removal of organic contaminants by carbon nanotubes, Sci. Total Environ. 482–483 (2014) 241–251.
[30] X. Tang, Q. Zhang, Z. Liu, K. Pan, Y. Dong, Y. Li, Removal of Cu(II) by loofah fibers as a natural and low-cost adsorbent from aqueous solutions, J. Mol. Liq. 199 (2014) 401–407.
[31] M.M. Nassar, Intraparticle diffusion of basic red and basic yellow dyes on palm fruit bunch, Water Sci. Technol. 40(7) (1999) 133–139.
[32] R.I. Yousef, B. El-Eswed, A.a.H. Al-Muhtaseb, Adsorption characteristics of natural zeolites as solid adsorbents for phenol removal from aqueous solutions: Kinetics, mechanism, and thermodynamics studies, Chem. Eng. J. 171(3) (2011) 1143–1149.
[33] B. Tanhaei, A. Ayati, M. Lahtinen, M. Sillanpää, Preparation and characterization of a novel chitosan/Al_2O_3/magnetite nanoparticles composite adsorbent for kinetic, thermodynamic and isotherm studies of Methyl Orange adsorption, Chem. Eng. J. 259 (2015) 1–10.
[34] M. Abdel Salam, M.A. Gabal, A.Y. Obaid, Preparation and characterization of magnetic multi-walled carbon nanotubes/ferrite nanocomposite and its application for the removal of aniline from aqueous solution, Synth. Met. 161(23–24) (2012) 2651–2658.
[35] S. Gupta, Theoretical and experimental investigations for removal of pollutants using adsorption (2008) Doctorial Thesis.